

Light-emitting diodes: a new paradigm for Ti:sapphire pumping

P. Pichon, Adrien Barbet, Jean-Philippe Blanchot, Frédéric Druon, François Balembois, Patrick Georges

► To cite this version:

P. Pichon, Adrien Barbet, Jean-Philippe Blanchot, Frédéric Druon, François Balembois, et al.. Light-emitting diodes: a new paradigm for Ti:sapphire pumping. *Optica*, Optical Society of America (OSA), 2018, 5 (10), pp.1236. 10.1364/OPTICA.5.001236 . hal-02193027

HAL Id: hal-02193027

<https://hal.archives-ouvertes.fr/hal-02193027>

Submitted on 24 Jul 2019

HAL is a multi-disciplinary open access archive for the deposit and dissemination of scientific research documents, whether they are published or not. The documents may come from teaching and research institutions in France or abroad, or from public or private research centers.

L'archive ouverte pluridisciplinaire **HAL**, est destinée au dépôt et à la diffusion de documents scientifiques de niveau recherche, publiés ou non, émanant des établissements d'enseignement et de recherche français ou étrangers, des laboratoires publics ou privés.

Light-emitting diodes : a new paradigm for Ti:sapphire pumping

PIERRE PICHON,^{1,2,*} ADRIEN BARBET,¹ JEAN-PHILIPPE BLANCHOT,²
FREDERIC DRUON,¹ FRANÇOIS BALEMBOIS¹ AND PATRICK GEORGES¹

¹Laboratoire Charles Fabry, Institut d'Optique Graduate School CNRS, Université Paris-Saclay, 91127, Palaiseau Cedex, France

²Effilux, 1 rue de Terre Neuve, 91940, les Ulis, France

*Corresponding author: pierre.pichon@institutoptique.fr

Received XX Month XXXX; revised XX Month, XXXX; accepted XX Month XXXX; posted XX Month XXXX (Doc. ID XXXXX); published XX Month XXXX

Ti:sapphire presents unequaled tuning properties. However, because of a short lifetime, the energy cannot be stored in Ti³⁺ upper level which makes this gain medium difficult to pump. Hence, the size, price and complexity of femtosecond laser chains are partially driven by their pump source. We present a novel concept to pump Ti:Sapphire based on light-emitting diodes (LEDs) which gathers ruggedness, compactness, simplicity and low price. Combining LEDs and a Ce:LuAG luminescent concentrator, we report the first LED-pumped Ti:sapphire laser. With 2240 blue LEDs (at 450 nm) in pulsed regime (10 Hz, 15 μ s), the pump module has a maximum emission at 530 nm and delivers up to 20.9 mJ with an irradiance of 9.9 kW/cm². This low-cost and compact pump system, among the brightest incoherent sources ever developed, enables a laser emission in Ti:sapphire (32 μ J at 790 nm). The tunability of the laser is demonstrated between 755 nm and 845 nm. The double pass small signal gain in the cavity is numerically simulated and measured to reach 1.066.

OCIS codes: (230.3670) Light-emitting diodes; (220.1770) Concentrators; (140.5560) Pumping; (140.3580) Lasers, solid-state; (140.3590) Lasers, titanium; (140.3600) Lasers, tunable.

<http://>

Titanium-doped sapphire (Ti:Al₂O₃) laser is at the center of femtosecond science with its unequaled emission bandwidth (>300 nm centered at 780 nm) allowing many applications in fundamental science, medicine and industry. The 130 nm wide absorption spectrum of this gain medium is centered on 490 nm and explains the great variety of light sources used to pump Ti:sapphire. In 1982, Moulton performed the first demonstration of a Ti:sapphire laser pumped with a 503 nm Coumarin 504 dye laser [1]. This first performance was quickly followed by other pump sources: flashlamp [2], 514 nm Argon-ion laser [3], 532 nm frequency doubled Nd:YAG laser [3-4] or Yb-doped fiber laser [5] and 511 nm copper vapor lasers [4]. Recently, research

efforts were oriented to simpler pump sources with semiconductors: frequency doubled laser diodes [6], optically pumped semiconductor lasers [7], direct 455 nm laser diode pumping [8-10] and direct 518 nm laser diode pumping [11].

The main issue for high energy femtosecond laser chains with Ti:sapphire is related to the pump energy for the amplifiers. Indeed, the very short lifetime of Ti³⁺ ions in sapphire (3 μ s at room temperature) strongly limits the potential energy storage by the gain medium. This means that the energy has to be stored in the pump systems and the pump light needs to be pulsed with energy ranging mJ-J with maximum pulse duration in the microsecond scale, close to the Ti:sapphire lifetime. Among the plethora of pump sources used for Ti:sapphire, only a few may address these requirements. The first ones, direct flashlamps, have been largely investigated in the past for high energy amplifiers [12]. However, the emission of few microsecond pulses requires the flashlamps to operate at very high current (kA) and very high voltage (kV), strongly reducing the lifetime operation and the repetition rate. Moreover, flashlamps emit a large spectrum with a significant part in the UV, inducing Ti:sapphire degradation (colored centers) and a poor spectral overlap with the absorption band of Ti:sapphire. This explains why flashlamps have rarely been used in Ti:sapphire commercial products.

The second pump sources addressing Ti:sapphire requirements are related to Nd-doped lasers. In case of flashlamp pumped Nd-doped lasers, the energy storage is shared between electrical devices for the flashlamps and the upper level of the laser medium, Nd³⁺ ions having a lifetime of several hundreds of μ s. In Q-switched operation and after frequency doubling, these sources deliver nanosecond pulses at the joule level at 532 nm (Nd:YAG) at low repetition rate (namely 10 Hz). Thanks to the development of high power laser diodes at 800 nm, driven by manufacturing applications, flashlamps have been progressively replaced by laser diodes for the pumping of low energy and high repetition rates systems. Despite the cost and complexity of these sources, frequency doubled neodymium doped lasers (Nd:YAG and Nd:YLF) have been the main pump sources for industrial Ti:sapphire systems for 25 years. They drove their size and their price and clearly limited their diffusion.

With the impressive development of GaN blue semiconductor sources, close to the absorption band of Ti:sapphire, a revisiting of the pump systems is relevant. However, high power blue and green laser

diodes have not known the same development than their counterpart in the near infrared: systems remain at the watt level even if the promising market of laser diode based projectors may drive their development in the future. Consequently, blue laser diodes are perfect for Ti:sapphire oscillators but they cannot afford Ti:sapphire pulse amplifiers with enough energy except with prohibitive cost and very complex systems.

The situation is completely different for blue light-emitting diodes (LEDs). Driven by massive research efforts for the lighting market, blue LEDs performance have experienced tremendous improvement with impressive cost reduction. In addition, LEDs are more rugged, simpler and much less sensitive to external environment than conventional laser diodes. With so cheap devices, energy storage can be considered with a massive collection of extremely simple components, each LED being driven at low current (A) and low voltage (V). To give an order of magnitude, it requires 10 000 LEDs emitting 1 W over 10 μ s to produce 100 mJ of blue light. Consequently, a pump module relying on a large number of LEDs shows an exceptional ruggedness as the damage of one LED will not significantly change the performance of the whole system.

However, LEDs are incoherent sources with limited irradiance: typically, in the order of 100 W/cm². This is enough to demonstrate the LED-pumping of Nd:doped lasers [13-17] but not for Ti:sapphire. Indeed, as transition metal doped gain medium, Ti:sapphire exhibits a very low $\sigma\tau$ product (namely emission cross section σ by lifetime τ), typically two orders of magnitude below Nd:doped materials. Hence, the irradiance of an LED is one order of magnitude below the requirements to reach the laser threshold of Ti:sapphire. A solution to overcome this problem is to combine LEDs with a luminescent concentrator (LC). This device has the property to circumvent the brightness conservation rule with a process of absorption/emission in a high index medium. Moreover, the slab geometry of an LED-pumped concentrator enables massive beam collection of elementary LEDs [18].

The first LED-pumped concentrator was reported with Ce:YAG [18], quickly followed by demonstrations for digital projection [19-22] and light sources in the yellowish [23]. They have been used to pump Nd:doped lasers [18,24] and an alexandrite laser [25]. In this paper, we reported the first LED-pumped Ti:sapphire laser using Ce:LuAG concentrators, chosen for the spectral matching with the absorption band of Ti:sapphire (Fig. 1).

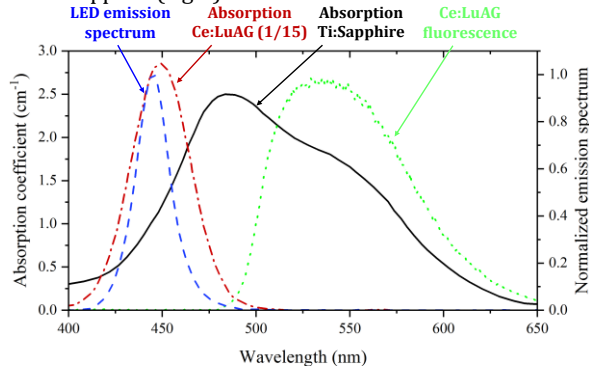


Fig. 1. Ce:LuAG (red), Ti:sapphire (black) absorption coefficients. Emission spectra of Ce:LuAG (green) and LED (blue) in the pulsed regime (15 μ s, 7 A, 10 Hz, room temperature).

To match the absorption band of Ce:LuAG, blue LEDs with an emission spectrum centered on 450 nm are used (LUXEON Z Royal Blue from Lumileds). This type of LED was chosen for its compactness: one LED package being 1.70 x 1.30 mm² for an emitting surface of 1 mm². At a maximum continuous current of 1 A, an LED emits 900 mW, corresponding to an irradiance of 90 W/cm². In pulsed regime, this

performance can be significantly improved: at 7 A during 15 μ s (close to Ti:sapphire lifetime), the peak LED irradiance increases to 425 W/cm². The LEDs' printed circuit board is mounted on a water-cooled heat sink. The 450 nm light from the LEDs is absorbed by Ce³⁺ ions and then reemitted within the concentrator (see the spectra on Fig. 1). The green light emitted in the concentrator is guided toward the edges of the concentrator via total internal reflections [18-25].

The key parameter to characterize an LED-pumped LC is the concentration factor introduced by Barbet et al [18] and defined by the ratio of the LC output radiance to a single pumping LED radiance. As LC are Lambertian sources, this is equivalent to the ratio of the LC irradiance to a single LED irradiance. The concentration factor depends on three parameters which are: the optical conversion efficiency, the aspect ratio of the luminescent concentrator (also called geometrical factor) and the LEDs filling factor of the pump facet. Our luminescent concentrator are slabs (14x1x100 mm³ in our case) proposing a large aspect ratio between the pump surface (14x100 mm²) and the emitting surface (1x14 mm²) corresponding to a geometrical factor of 200. The thickness of the concentrator has been set to 1 mm so that all blue light from LEDs is absorbed. 1120 LEDs are used to pump one luminescent concentrator (560 LEDs on each 14x100 mm² facets). In this configuration, the filling factor reaches 41% (meaning that 41% of the pump facets is filled with an LED emitting surface).

Pulsing the LEDs at 10 Hz with a duration of 15 μ s and a current up to 7 A, the measured output peak irradiance at the LC surface (1x14 mm²) is 2.6 kW/cm² in air and 6.6 kW/cm² using an index-matching optical adhesive to couple the light in the Ti:sapphire crystal (Norland Product, inc NOA170 with a refractive index of 1.7). The optical conversion efficiency of the concentrator is then respectively 7.8% and 19%, corresponding to a concentration factor of 6.4 and 15. This means that the LC has a radiance higher than an LED by a factor 15. Hence, with the beam collection of 1120 LEDs, the LC is able to provide green flashes with an energy of 13.9 mJ over 15 μ s (see Table 1).

Table 1: Properties and performance of the Ce:LuAG luminescent concentrators studied in this work

Number of Ce:LuAG	1		2		
	Dimension (mm ³)		1 x 14 x 100		1 x 14 x 200
Output facet configuration	Air	With index coupling	Air	With index coupling	
Output Peak Power (kW)	0.364	0.924	0.546	1.386	
Output Irradiance (kW/cm ²)	2.6	6.6	3.9	9.9	
Output Radiance (kW/cm ² /sr)	0.828	2.1	1.24	3.15	
Energy (15 μ s, 10 Hz) (mJ)	5.46	13.9	8.16	20.9	
Optical efficiency (%)	7.8	19	5.8	14	
Filling factor (%)	41		41		
Geometrical factor	200		400		
Concentration factor	6.4	15	9.5	23	

The energy scaling of this pumping system is performed bonding a second luminescent concentrator to the first one with an index matching UV curing optical adhesive. Thus, 2240 LEDs are used to pump a 200-mm-composit luminescent concentrator exhibiting a

geometrical factor of 400. In the same mode of operation as described previously, the output irradiance measured at the 200 mm long LC surface is 3.9 kW/cm^2 in air and 9.9 kW/cm^2 using an index-matching optical adhesive. Thus, adding a second LC module to the first one only increases by 50% the pump irradiance mainly due to the interface between the two LC. The optical conversion efficiency of the concentrator is then 5.8% and 14% for a concentration factor of 9.5 and 23, respectively. The radiance reaches $1240 \text{ W/cm}^2/\text{sr}$ in air and $3150 \text{ W/cm}^2/\text{sr}$ in the Ti:sapphire crystal, in the same order of magnitude than the radiance of flashlamps. This corresponds to an energy of 20.9 mJ that can be delivered to the Ti:sapphire crystal.

The 200-mm-long composite LED-pumped luminescent concentrator is now used to pump a Ti:sapphire crystal. The gain medium is $1 \times 1 \times 14 \text{ mm}^3$, matching with the luminescent concentrator output facet (Fig. 2), and directly bonded to the luminescent concentrator with a UV curing optical adhesive. The laser gain medium is 0.25 at% Ti-doped and oriented such that the pump arrives on a Ti:sapphire surface parallel to the c-axis in order to maximize absorption. One of the laser crystal longitudinal surfaces is high-reflectivity coated over 780-820 nm, the opposite surface being anti-reflection coated for the same wavelength range. A plano-concave, 54-mm-long laser cavity is designed with 300-mm radius-of-curvature output couplers having different transmissions: 1.0%, 2.0% and 2.8% at the lasing wavelength.

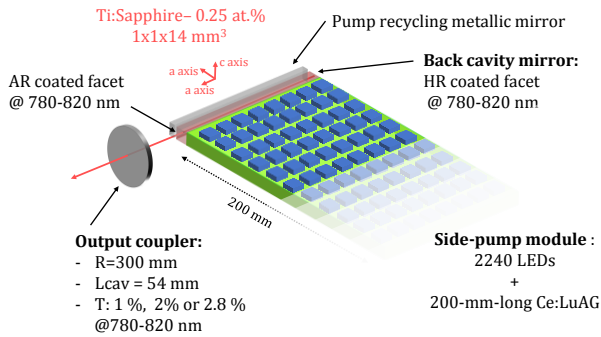


Fig. 2. Setup of the experiment.

LEDs are pulsed at 10 Hz with a current of 7 A for 15 μs . In this mode of operation, Ti^{3+} ions lifetime is measured to reach 2.6 μs corresponding to a temperature of 53 $^\circ\text{C}$ [3]. 43% of the injected pump energy is absorbed by a single pass in the 1 mm Ti:sapphire crystal. In order to increase the absorption, two mirrors (metallic 80% reflectivity) were placed behind the laser crystal and at the unused facet of the luminescent concentrator (Fig. 2). With this setup, the unabsorbed pump energy is re-injected into the gain media and is reflected between the two metallic mirrors until it is either absorbed by the gain medium or lost (mirror absorption or Ce:LuAG reabsorption). The pump absorption improvement is measured by investigating the fluorescence of Ti:sapphire which is linearly correlated to the absorbed energy. It has been measured that the pump recycling improves by 60% the absorption. This means that 14.4 mJ are absorbed by the gain media over the 20.9 mJ delivered by the pump module.

The laser output energy as a function of the pump energy delivered by the luminescent concentrator is plotted on Fig. 3 (a) for a 1.0%, 2.0% and 2.8% output couplers. A maximum laser energy of 32 μJ at 790 nm (Fig. 3 (a) inset) has been reached with the 2.0% transmission output coupler. The beam quality was measured to be $M_x^2=6.5$ in the horizontal direction and $M_y^2=3$ in the vertical direction (Fig. 3 (b) inset). The laser operates during 10.8 μs with a buildup time of 4.2 μs (Fig. 3 (b)). For a pump energy of 20.9 mJ from the LC, the optical efficiency is then 0.15%.

The total energy emitted by the 2240 LEDs is 143 mJ, which corresponds to a global efficiency of 0.023%.

After careful alignment of the cavity, we achieved TEM_{00} operation, the highest laser output energy reached 18 μJ with a 2% transmission output coupler.

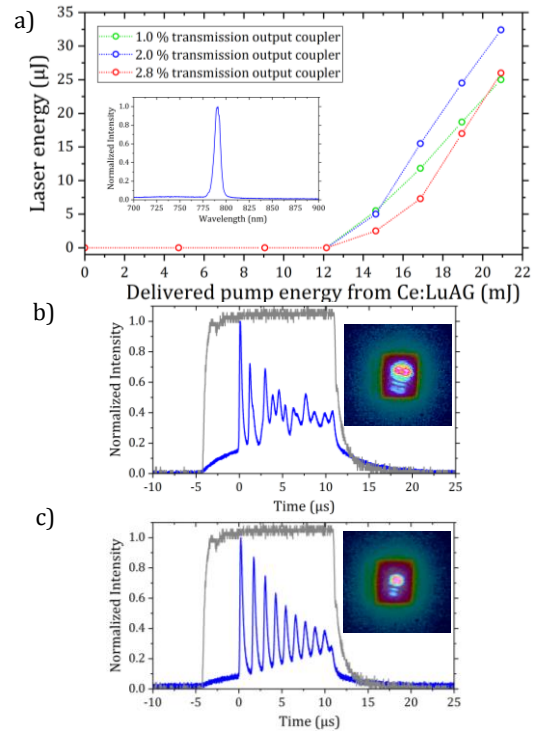


Fig. 3. a) Laser output energy at 790 nm versus the pump energy delivered by the luminescent concentrator for 1.0%, 2.0% and 2.8% transmissions output couplers. Inset: laser spectrum in free running operation. b) Laser and fluorescence temporal profiles in multimode operation. The LEDs pump pulse is overlaid with the grey curve. Insets: spatial profile of the laser overlaid with the fluorescence of the $1 \times 1 \text{ mm}^2$ emitting facet of the Ti:sapphire crystal. c) Temporal and spatial profiles of the TEM_{00} mode.

The tunability of the laser is investigated inserting an SF10 prism in an extended cavity (125-mm-long). The laser output power versus the laser wavelength is plotted on Fig. 4. The tunability of the laser is performed between 755 nm and 845 nm with a maximum emission at 800 nm limited by the coating of the two couplers of the cavity. As the laser cavity must be extended in order to insert the prism, it results in lower output energies: a consequence of the smaller laser mode in the gain medium since the radius of curvature of the output coupler is no longer optimized for this cavity size.

The small signal gain per double pass is measured by investigating at the laser threshold as a function of intracavity calibrated Fresnel losses [26]. The losses are controlled by an intracavity 8 mm thick N-BK7 flat window with a variable incidence angle around the Brewster angle. The measurements are performed with a 120-mm-long cavity and a 2% output coupler. The roundtrip passive losses measured with the Findlay-Clay method reaches 9.4% [27] attributed to reabsorption losses in the near infrared and the anti-reflective coating of the Ti:sapphire.

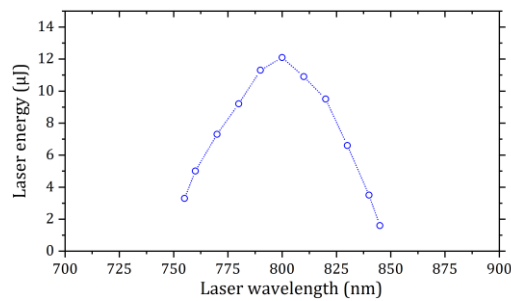


Fig. 4. Laser output power versus laser wavelength. Performed with an SF10 prism in a 125-mm-long cavity.

For a pump energy of 20.9 mJ, a double pass small signal gain of 1.066 is measured (Fig. 5). The small signal gain per double pass is numerically simulated using a local estimation of the pump density in the gain medium and properties of Ti:sapphire directly measured on the sample used in this study (absorption of Ti:sapphire and Ti^{3+} ions lifetime). The estimation of the pump density is performed with a ray tracing software based on the Monte-Carlo algorithm (LightTools®).

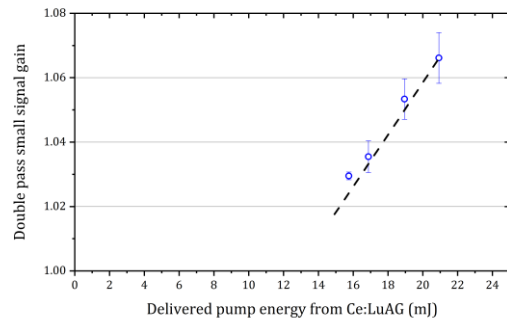


Fig. 5. Small signal gain per double-pass versus the pump energy: numerically simulated (dashed line) and measured with a 1% output coupler (dots).

In conclusion, we demonstrated a new pump source for Ti:sapphire relying on blue LEDs and Ce:LuAG luminescent concentrators. It has a radiance higher by a factor 23 compared to an LED which is the highest concentration value ever reached. This easily power-scalable pump source, emitting at 530 nm, delivers a radiance up to 9.9 kW/cm^2 . To our best knowledge, this Ce:LuAG concentrator is among the brightest incoherent sources ever developed. It is a very promising light source in the visible as its emission spectrum corresponds to the semiconductor's green gap and opens the way for many applications in vision and fluorescent microscopy.

Laser operation with Ti:sapphire is clearly demonstrated and understood with significant output energy ($32 \mu\text{J}$), gain (1,066) and tunability (755-845 nm). Even if the efficiency remains modest, this work brings the proof of concept of the suitability of LED pumped LC for Ti:sapphire.

A major asset of LED-pumped LCs is energy scaling (related to LC width scaling) and massive collective operation assuring long lifetime, stability and robustness. Further pump energy scaling can be imagine starting with pumping unused facets of the gain medium (potentially designing a polygonal Ti:sapphire), considering new luminescent crystals having a better spectral matching between the LC and the gain medium and using the advantage of side pumping with a longer gain medium.

LED-pumped LCs may open the way to a more compact, rugged, simpler and less expensive generation of amplifiers in Ti:sapphire femtosecond laser chain that will benefit to all scientific, industrial and

medical applications. This work only represents the first step toward this target.

Funding. Agence Nationale de la Recherche and Direction Générale de l'Armement (ANR-17-ASTR-0021)

REFERENCES

1. P. F. Moulton, *Opt. News*, **8**, 9, (1982).
2. L. Esterowitz, R. Allen, and C. P. Khattak, *Tunable Solid-State Lasers*, Springer Ser. in Opt. Sci., **47**, 73, (1985).
3. P. F. Moulton, *J. Opt. Soc. Am. B*, **3**, 125, (1986).
4. K. Takehisa and A. Miki, *Applied Optics*, **31**, 2734, (1992).
5. G. K. Samanta, S. Chaitanya Kumar, K. Devi, and M. Ebrahim-Zadeh, *Opt. Laser Eng.*, **50**, 215, (2012).
6. A. Müller, O. Jensen, A. Unterhuber, T. Le, A. Stingl, K. Hasler, B. Sumpf, G. Erbert, P. Andersen, and P. Petersen, *Opt. Express*, **19**, 12156, (2011).
7. B. Resan, E. Coadou, S. Petersen, A. Thomas, P. Walther, R. Viselga, J-M. Heritier, J. Chilla, W. Tulloch and A. Fry, *Proc. SPIE 6871, Solid State Lasers XVII: Technology and Devices*, 687116, (2008).
8. P. Roth, A. Maclean, D. Burns, and A. Kemp, *Opt. Lett.*, **34**, 3334, (2009).
9. Charles G. Durfee, Tristan Storz, Jonathan Garlick, Steven Hill, Jeff A. Squier, Matthew Kirchner, Greg Taft, Kevin Shea, Henry Kapteyn, Margaret Murnane, and Sterling Backus, *Opt. Express*, **20**, 13677 (2012).
10. S. Backus, M. Kirchner, R. Lemons, D. Schmidt, C. Durfee, M. Murnane and H. Kapteyn, *Opt. Exp.*, **25**, 3666 (2017).
11. S. Sawai, A. Hosaka, H. Kawauchi, K. Hiroswawa and F. Kannari, *Applied Physics Express*, **7**, 022702, (2014).
12. A. Hoffstadt, *IEEE J. of Quant. Elec.*, **30**, 1850 (1997).
13. A. Barbet, F. Balembois, A. Paul, J-P. Blanchot, A-L. Viotti, J. Sabater, F. Druon and P. Georges, *Opt. Lett.*, **39**, 9731 (2014).
14. B. Villars, E. Hill and C. Durfee, *Opt. Lett.*, **40**, 3049 (2015).
15. K-Y. Huang, C-K. Su, M-W. Lin, Y-C. Chiu and Y-C. Huang, *Opt. Exp.*, **24**, 12043, (2016).
16. C-Y. Cho, C-C. Pu, K-W. Su and Y-F. Chen, *Opt. Lett.*, **42**, 2394 (2017).
17. Simon J. Herr, Karsten Buse, and Ingo Breunig, *Photon. Res.*, **5**, B34, (2017)
18. A. Barbet, A. Paul, T. Gallinelli, F. Balembois, J.-P. Blanchot, S. Forget, S. Chénais, F. Druon, and P. Georges, *Optica*, **3**, 465, (2016).
19. S. Roelandt, Y. Meuret, D. de Boer, D. Bruls, P. Van de Voorde, H. Thienpont, *Opt. Eng.*, **54**, 55101, (2015).
20. D. de Boer, D. Bruls, H. Jagt, *Opt. Exp.*, **24**, A1069, (2016).
21. D de Boer, D Bruls, C. Hoelen, H. Jagt, *Proc. of SPIE 10378, 103780M-1* (2017).
22. C. Hoelen, P. Antonis, D. de Boer, R. Koole, S. Kadijk, Y. Li, V. Vanbroekhoven, P. Van de Voorde, *Proc. of SPIE 10378, 103780N-1* (2017).
23. J. Sathian, J. Breeze, B. Richards, N. McN. Alford and M. Oxborrow, *Opt. Exp.*, **25**, 13714, (2017).
24. P. Pichon, A. Barbet, P. Legavre, T. Gallinelli, F. Balembois, J.-P. Blanchot, S. Forget, S. Chénais, F. Druon, and P. Georges, *Opt. and Laser Tech.*, **96**, 7, (2017).
25. P. Pichon, A. Barbet, F. Druon, J.-P. Blanchot, F. Balembois, and P. Georges, *Opt. Lett.*, **42**, 4191, (2017).
26. F. Balembois, F. Falcoz, F. Kerboull, F. Druon, P. Georges, and A. Brun, *IEEE J. Quantum Electron.*, **33**, 1614, (1997).
27. D. Findlay and R. Clay, *Phys. Lett.*, **20**, 277, (1966).